nature microbiology

ARTICLES

https://doi.org/10.1038/s41564-018-0161-3

Distinct mechanisms coordinate transcription and translation under carbon and nitrogen starvation in *Escherichia coli*

Sukanya Iyer[1], Dai Le[1], Bo Ryoung Park[1] and Minsu Kim[1,2,3]*

Bacteria adapt to environmental stress by producing proteins that provide stress protection. However, stress can severely perturb the kinetics of gene expression, disrupting protein production. Here, we characterized how *Escherichia coli* mitigates such perturbations under nutrient stress through the kinetic coordination of transcription and translation. We observed that, when translation became limiting under nitrogen starvation, transcription elongation slowed accordingly. This slowdown was mediated by (p)ppGpp, the alarmone whose primary role is thought to be promoter regulation. This kinetic coordination by (p)ppGpp was critical for the robust synthesis of gene products. Surprisingly, under carbon starvation, (p)ppGpp was dispensable for robust synthesis. Characterization of the underlying kinetics revealed that under carbon starvation, transcription became limiting, and translation aided transcription elongation. This mechanism naturally coordinated transcription with translation, alleviating the need for (p)ppGpp as a mediator. These contrasting mechanisms for coordination resulted in the condition-dependent effects of (p)ppGpp on global protein synthesis and starvation survival. Our findings reveal a kinetic aspect of gene expression plasticity, establishing (p)ppGpp as a condition-dependent global effector of gene expression.

Bacteria adapt to environmental stress by modulating gene expression[1]. For example, in response to starvation, bacteria produce proteins to detoxify, strengthen the cell envelope or scavenge other potential nutrient sources[2–5]. In response to osmotic stress, they produce osmo-protectant transporters[6]. Robust production of such proteins is essential for cell survival under conditions of stress, but is a challenging task, as stress has detrimental effects on gene expression processes. For example, starvation causes dimerization of ribosomes, which, known as ribosomal hibernation, reduces their activities[7]. Osmotic stress triggers the dissociation of RNA polymerases (RNAPs) from DNA templates[8]. Such molecular events adversely perturb gene expression kinetics. Such perturbations, if left unchecked, will disrupt protein production and impair cell survival. Currently, it is unclear how cells cope with such perturbations and ensure robust protein production.

Gene expression is an intricately coordinated multistep process. In bacteria, as RNAPs begin to transcribe a gene, ribosomes immediately load onto and translate the nascent mRNAs[9]. The close trailing of ribosomes behind RNAPs is critical for robust gene expression; if not, transcription becomes terminated prematurely, for example by the transcription terminator factor Rho[10], resulting in failure to synthesize full-length mRNAs and functional proteins (see Supplementary Fig. 1 caption for details). Thus, transcription and translation must be coordinated, and any perturbations that disrupt this coordination can have deleterious effects on gene expression. Therefore, to understand how cells ensure robust gene expression under stress conditions, systematic characterization of transcriptional and translational kinetics is essential. In particular, mechanisms coordinating these kinetics must be extensively characterized.

In this work, we systematically characterized transcriptional and translational kinetics in *E. coli* cells starved of carbon or nitrogen. This type of nutrient stress was chosen because bacteria in nature are often starved of carbon or nitrogen[11], and starved bacteria can robustly express genes[5,12–14], suggesting the existence of mechanisms coordinating transcription and translation. Recently, we developed a sensitive mRNA quantification technique based on single-molecule fluorescence in situ hybridization (smFISH)[15]. Combining this technique with the β-galactosidase assay and quantitative modelling, we conducted absolute quantification of kinetic parameters, for example transcriptional/translational rates and elongation speeds. Furthermore, because the disruption of transcription–translation coordination results in premature transcription termination (failure to synthesize full-length mRNAs), we separately characterized the head and tail parts of mRNAs.

Results

Significant perturbations of transcription kinetics by C starvation and translation kinetics by N starvation.. Upon exposure to stress, bacteria activate relevant promoters[1], and the robust synthesis of gene products following promoter activation is critical for survival. Complex molecular regulations of promoter activation have been previously studied by others. In this study, we wished to focus on the processes that follow promoter activation, namely synthesis of gene products, and avoid the complications caused by complex promoter regulation. Therefore, we used a synthetic promoter, $P_{LTet\text{-}O1}$, which can be activated by an artificial inducer, aTc. In our *E. coli* strain (NMK80), $P_{LTet\text{-}O1}$ drives the expression of a *lacZ* reporter gene in its chromosome (Supplementary Fig. 2a).

We cultured this strain in minimal medium with glycerol and ammonium as the sole carbon and nitrogen sources, respectively (C+ N+ condition). We then starved it of either glycerol (C starvation) or ammonium (N starvation). At the onset of starvation, cell growth abruptly stops, which defines time 0 (Supplementary Fig. 3). Then, 100 ng ml^{-1} of aTc was added to the culture (Supplementary Fig. 2b). Previous studies showed that protein expression is most active within

[1]Department of Physics, Emory University, Atlanta, GA, USA. [2]Graduate Division of Biological and Biomedical Sciences, Emory University, Atlanta, GA, USA. [3]Emory Antibiotic Resistance Center, Emory University, Atlanta, GA, USA. *e-mail: minsu.kim@emory.edu

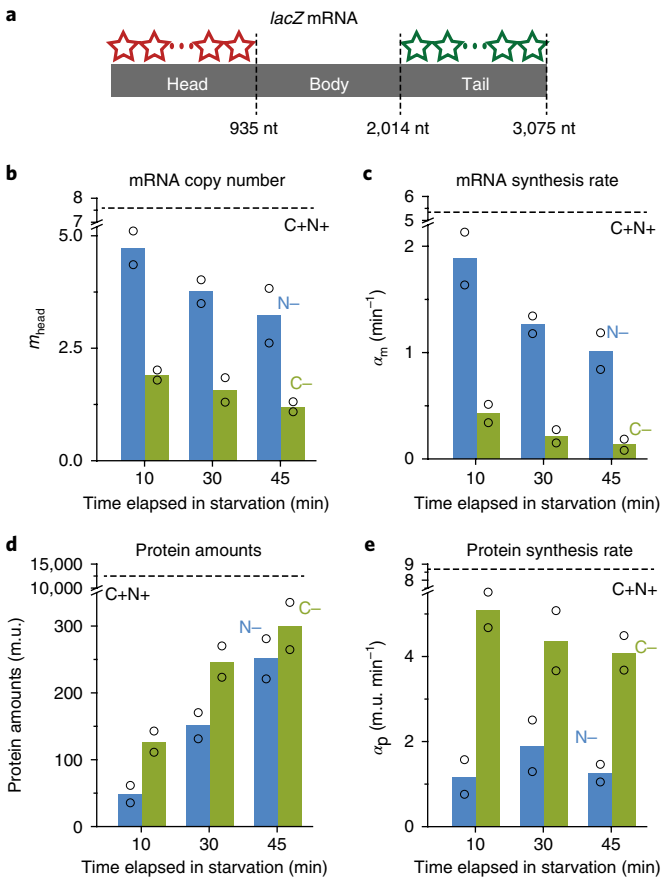

Fig. 1 | Effects of C- and N starvation on gene expression kinetics. a, We detected single *lacZ* mRNA molecules using smFISH. We hybridized the head and tail of the mRNA molecule with probes labelled with two different fluorescent dyes (ATTO 647 N and TAMRA, respectively). **b**, Quantitative analysis of hybridization signals yielded the average copy number of the mRNA head per cell, m_{head} (plotted here). The copy number of the mRNA tail, m_{tail}, was similar to m_{head} (Supplementary Fig. 5). **c**, By analysing a linear increase in mRNA amounts after promoter induction, we determined the mRNA synthesis rate, α_m; see Supplementary Fig. 7 for detail. **d**, We determined LacZ protein amount using the β-galactosidase assay. **e**, By analysing an increase in protein amounts after promoter induction, we determined the rate of protein synthesis from a single mRNA molecule, α_p; see Supplementary Fig. 9 for detail. In these figures, the dashed line, blue columns on the left, and green columns on the right indicated the measured values for C+N+ cells, N-starved cells, and C-starved cells, respectively. In all cases, two biologically independent experiments were performed. The dots and bar show the data from the two independent experiments and their mean. The actual values of all kinetics parameters are reported in Supplementary Table 1.

the first hour of starvation, and the expression during this early hour is important for long-term survival[5]; see Supplementary Information 1 for details. Accordingly, the present investigation focused on gene expression during the first hour of starvation. In this experimental time window, viability loss is negligible (Supplementary Fig. 4).

We labelled the head and tail of *lacZ* mRNA molecules with different fluorescent dyes and measured mRNA amounts; see Fig. 1a, Methods, and Iyer et al.[15]. The average copy number of the mRNA head per cell, m_{head}, was ~7.5 in the C+N+ condition and was reduced by ~2-fold under N starvation, and by ~4-fold under C starvation (Fig. 1b). We made a similar observation for the mRNA tail, m_{tail} (Supplementary Fig. 5). These and other values obtained from this study are provided in Supplementary Table 1.

The mRNA amounts are determined by the mRNA synthesis rate, α_m, and degradation rate, β_m, as described in Supplementary Equation (1); see Supplementary Fig. 6 caption. We first sought to test whether the mRNA amounts were lower in C-starved cells because mRNAs were degraded more rapidly (higher β_m). However, β_m was actually lower in C-starved cells; ~0.2 min^{-1}, compared to ~0.5 min^{-1} for C+N+ and N-starved cells (Supplementary Fig. 6 and Table 1). Next, we determined the mRNA synthesis rate α_m by analysing a linear increase in mRNA amounts after promoter induction; see Supplementary Equation (3) in Supplementary Fig. 7. We found that α_m in C-starved cells was lower than that in N-starved cells by approximately fourfold (Fig. 1c); see Supplementary Fig. 7 for details. Therefore, C starvation limited mRNA synthesis more severely than did N starvation. This approximately fourfold lower synthesis rate in C-starved cells, together with their approximately twofold lower degradation rate (Supplementary Fig. 6), predicts that their mRNA amounts should be approximately twofold lower than those of N-starved cells. This prediction agrees with our observation above (Fig. 1b), showing internal consistency.

We next characterized LacZ protein expression using the β-galactosidase assay. This assay reports the amounts in Miller units (m.u.); 1 m.u. corresponds to ~0.5 LacZ tetramers/cell[16]. Figure 1d shows that LacZ protein amounts were lower under N starvation than under C starvation.

Protein amounts (p) are determined by the number of mRNA molecules (m), rate of protein synthesis from a single mRNA molecule (α_p) and rate of protein degradation (β_p), as described in Supplementary Equation (4); see Supplementary Fig. 9 caption. Our measurements of LacZ amounts after complete inhibition of LacZ synthesis revealed no LacZ degradation ($\beta_p = 0$) in C-starved or N-starved cells (Supplementary Fig. 8). Then, the lower protein amounts in N-starved cells (Fig. 1d), despite higher mRNA amounts (Fig. 1b), must be due to a lower rate of protein synthesis α_p. We next directly determined α_p by analysing an increase in protein amounts after promoter induction; see Supplementary Fig. 9 for details. Figure 1e shows that α_p was significantly lower in N-starved cells than in C-starved cells (~4.5 versus ~1.5 m.u. min^{-1}), agreeing with our expectation. Thus, N starvation limited protein synthesis more severely than did C starvation. This result is in contrast with our previous observation that C starvation limited mRNA synthesis more severely than did N starvation (Fig. 1c).

Motivated by the severe effect of C starvation on mRNA synthesis (Fig. 1c), we next investigated the effect of C starvation on transcription elongation. We determined the mRNA chain elongation speed by characterizing a time delay in the appearance of mRNA segments; see Supplementary Fig. 7 and our recent article[15] for details. We obtained 48 nt s^{-1} for C+N+ cells, which is in agreement with ~45 nt s^{-1} reported in the literature[17,18]. In C-starved cells, the speed was reduced by more than 2-fold (23.3, 16.9 and 12.9 nt s^{-1} for 10, 30 and 45 min starvation, respectively), further showing a repressive effect of C starvation on transcription. This effect is represented by the green line in Fig. 2a.

Contrary to C starvation, N starvation severely reduced the protein synthesis rate (Fig. 1e). We next investigated the effect of N starvation on translation elongation by measuring a time delay in the appearance of the LacZ protein after induction; see previous studies[18–22] and Supplementary Fig. 9 for details of the measurement. We found that the peptide chain elongation speed in C+N+ cells was 12.9 amino acids per second, which agrees with ~14 amino acid per second reported in the literature[18–22]. Under N starvation, the speed was reduced by more than 2-fold (4.1, 5.2, and 5.3 amino acid per second for 10, 30, and 45 min starvation, respectively), further showing a repressive effect of N starvation on translation. This effect is represented by the blue line in Fig. 2b.

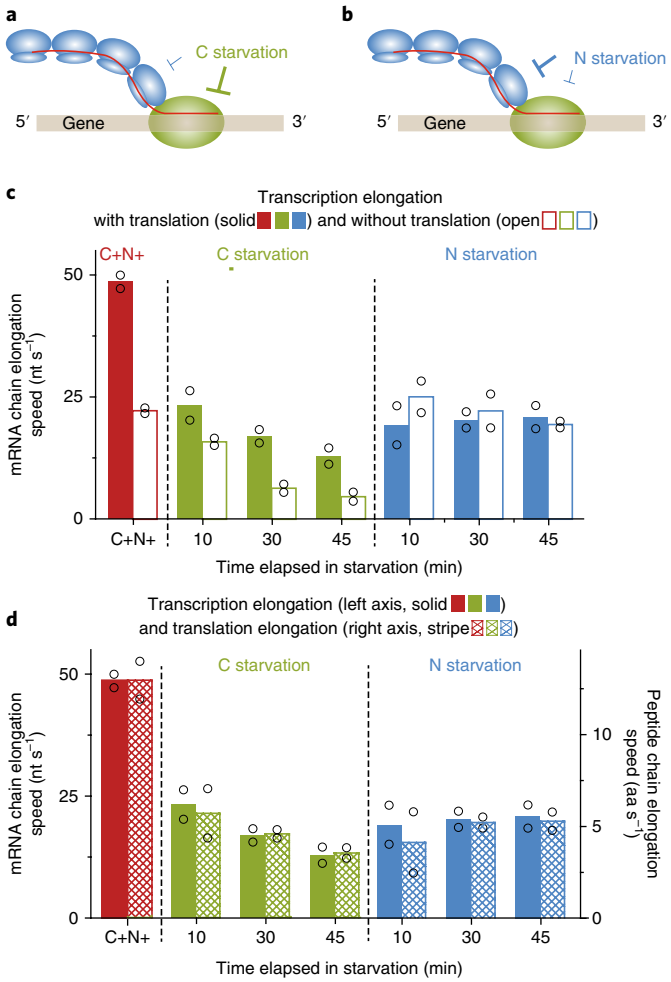

Fig. 2 | Characterization of transcription elongation and translation elongation. a,**b**, Illustration of transcription by RNAPs (green circles) and translation by ribosomes (blue circles). As RNAPs synthesize nascent mRNAs (red line), ribosomes closely trail the RNAPs and translate. Our findings indicated that C starvation limits transcription more strongly (**a**), while N starvation limits translation more strongly (**b**); see text. **c**, We compared the *lacZ* mRNA chain elongation speeds with translation (solid columns) and without translation (open columns) for C+N+ cells (red on the left) and C-starved cells (green in the middle), and N-starved cells (blue on the right). See Supplementary Note 2 for further discussion. **d**, We compared the *lacZ* mRNA chain elongation speeds (solid columns, left axis) and LacZ peptide chain elongation speeds (striped columns, right axis). The scales of the axes were adjusted such that the heights of the two columns matched for C+N+ cells (red). We then plotted those speeds for C-starved cells in the middle (green) and for N-starved cells to the right (blue). We note that we generally experienced larger experimental errors in measurements of cells starved for 10 min. This is possibly because the uncertainty in determining the onset of starvation is about 10 min, which is comparable to the duration of the starvation for the cells. In all cases, two biologically independent experiments were performed. The dots and bar show the data from the two independent experiments and their mean.

Under the transcription-limiting C starvation condition, the 'translation-aid-transcription' mechanism naturally coordinates transcription to translation.. Next, we characterized the coordination of transcription elongation and translation elongation. As discussed in the introduction, for bacteria in nutrient-rich conditions, these elongation kinetics are tightly coordinated[9]: transcribing RNAPs (forerunners) are closely trailed by translating ribosomes (followers). The loss of this coordination (which occurs when ribosomes lag behind RNAPs) leads to premature transcription termination (Supplementary Fig. 1 caption). Previous studies showed that in nutrient-rich conditions, coordination is naturally maintained by the 'translation-aid-transcription' mechanism[18]. The transcriptional motion of the forerunner, RNAP, is slow due to its spontaneous pausing and backtracking[23–25], whereas the translational motion of following ribosomes is highly processive[26]. Thus, the followers (ribosomes) catch up with and push forward the forerunner (RNAPs), speeding up transcription elongation[18]. The key evidence for this mechanism is a substantial slowdown of transcription elongation when translation is inhibited[18].

We first replicated this evidence in our C+N+ cells. Following the procedure of the previous study[18], we treated cells with chloramphenicol, an inhibitor of peptide-chain elongation. We indeed observed a significant effect of translation on transcription. Without translation inhibition, the *lacZ* mRNA chain elongation speed was 48.6 nt s^{-1} (red solid, Fig. 2c); this was the speed when aided by translation. With inhibition, the speed was reduced to 22.3 nt s^{-1} (red open, Fig. 2c); this was the speed when unaided by translation. This faster transcription elongation when aided by translation, consistent with the previous finding[18], indicates that the translation-aid-transcription mechanism is in effect in C+N+ cells.

As illustrated in Fig. 2a, C starvation retards the transcriptional motion of RNAPs; see approximately twofold reduction in speed in C-starved cells compared to C+N+ cells (Fig. 2c). With slow motion of the forerunner, RNAP, the translation-aid-transcription mechanism would remain in effect under C starvation. This means that the mRNA chain elongation speeds we found above for C-starved cells were likely to be the values upheld by aiding translation. To determine the speed when unaided, we inhibited translation using chloramphenicol. With inhibition, the speed was reduced (green, Fig. 2c), for example from 16.9 to 6.4 nt s^{-1} for 30 min starvation. This speed is several-fold lower than the speed we found for translation-inhibited C+N+ cells (22.3 nt s^{-1} in Fig. 2c), further highlighting a severe limitation of C starvation on transcription. Importantly, the faster transcription elongation with translation suggests that the translation-aid-transcription mechanism is in effect in C-starved cells.

To provide further support for this mechanism in C-starved cells, we next compared transcription and translation elongation. The translation-aid-transcription mechanism naturally ensures coordination between transcription and translation elongation[9]. Therefore, when cells in C+N+ condition are subjected to C starvation and transcription elongation becomes slow (Fig. 2a), translation elongation must slow down by the same degree. We tested this possibility by comparing C+N+ and C-starved cells. First, in Fig. 2d, we plotted the mRNA chain elongation speed (solid, left axis), and peptide chain elongation speed (striped, right axis) for C+N+ cells (red). We then plotted the mRNA chain elongation speed for C-starved cells (green solid column); the reduced height of this column reflects the expected slow-down in transcription elongation under C starvation. When we plotted the peptide chain elongation speed for C-starved cells (green striped column), the heights of these green columns remained matched (Fig. 2d), indicating that translation elongation indeed slowed down by the same degree.

Under the translation-limiting N starvation condition, transcription is not aided by translation, and yet transcription remains coordinated to translation.. The critical requirement for the translation-aid-transcription mechanism is the fast translation motion of ribosomes (followers). In translation-limiting conditions such as N starvation (Fig. 2b), this requirement may not be satisfied. Indeed, previous studies showed that under amino acid starvation, ribosomes stall and are decoupled from transcribing RNAPs[27]. When such decoupling occurs, the translation-aid-transcription mechanism would no longer be in effect. To test this possibility, we

repeated the translation inhibition experiments using chloramphenicol under N starvation. Our experiments above using C-starved and C+N+ cells showed that translation inhibition led to significantly slower transcription elongation (red and green in Fig. 2c), revealing the translation-aid-transcription mechanism in them. In contrast, in N-starved cells, transcription elongation was similar with and without inhibition, suggesting that translation does not aid transcription in N-starved cells; see blue columns in Fig. 2c (and also Supplementary Fig. 10).

Translation cannot aid transcription if the ribosomes (followers) lag behind RNAPs (forerunners), that is, loss of transcription–translation coordination. We wondered if this loss of coordination occurred under N starvation. As discussed above (and also in Supplementary Fig. 11), the hallmark of this loss of coordination is premature termination of transcription. When we re-examined our previous data (Supplementary Fig. 7), however, N-starved wild-type (WT) cells synthesized the mRNA tail almost as well as the head. This lack of premature termination suggests that transcription remains coordinated to translation. To further support this coordination, we compared their elongation speeds; if coordinated, when N starvation retards translation elongation, transcription elongation must slow down by the same degree. We observed in Fig. 2d that at 10 min of starvation, the latter was marginally higher than the former, although the difference is well within measurement errors. For cells starved for 30 min or 45 min, mRNA chain elongation and peptide chain elongation speeds matched. These data, together with the absence of premature termination, indicate that transcription remains coordinated to translation in N-starved cells.

Mechanism of coordinating transcription to translation under N starvation.. The translation-aid-transcription mechanism naturally ensures the coordination of transcription to translation[9]. Interestingly, our results above indicate that transcription and translation remain coordinated even when this mechanism is no longer in effect under translation-limiting N starvation. What is the mechanism underlying this coordination? When translation elongation becomes slow, the only way to maintain the coordination is to also slow down transcription elongation. The consideration of which factor may be involved in this process led us to previous inconclusive results concerning nucleotide guanosine (penta) tetraphosphate, (p)ppGpp, the central molecule for adaptation to starvation[28]. (p)ppGpp accumulates in large amounts in cells upon starvation, for example an approximately tenfold increase in concentration upon N starvation[29], C starvation[30,31] or other modes of starvation[32–34]. Its accumulation represses the synthesis of rRNA and other proteins[28]. Studies in the 1980s and 1990s reported that (p)ppGpp induction slowed down transcription elongation[35–39]. These early studies attempted to attribute the repression of rRNA synthesis by (p)ppGpp to this slow-down. However, this attempt was invalidated after later studies confirmed that the repression was caused by the direct inhibition of promoters by (p)ppGpp (for example, see[40–43]). Subsequently, more recent work has failed to demonstrate significant slow-down of transcription elongation by (p)ppGpp, challenging the findings of the former studies[44]. Currently, what role (p)ppGpp plays in gene expression kinetics is unclear.

Under N starvation, (p)ppGpp plays a central role in coordinating transcription to translation.. We wondered if this role of (p)ppGpp remains unclear because it is condition dependent. If so, this role must be considered in the context of specific starvation conditions. Thus, we first characterized this role under N starvation. As noted above, in translation-limiting conditions, transcription must slow down to stay coordinated with translation. We hypothesized that under the translation-limiting N starvation condition, (p)ppGpp slows down transcription elongation, thereby coordinating transcription with translation. We tested this hypothesis below by controlling (p)ppGpp synthesis and characterizing gene expression kinetics.

We first induced (p)ppGpp synthesis in C+N+ cells and determined how the mRNA chain elongation speed changed. In *E. coli*, (p)ppGpp molecules are synthesized by RelA (with synthesis activity only) and SpoT (with synthesis and hydrolysis activities)[28]. We introduced a plasmid containing P_{tac}-relA′, pALS13[45] into our *E. coli* strain (NMK156); note that RelA′ has a strong (p)ppGpp synthesis activity, and its expression can be activated using the inducer IPTG. The induction of (p)ppGpp synthesis led to an approximate twofold reduction in mRNA chain elongation speed (Supplementary Fig. 12).

Starvation induces (p)ppGpp accumulation[29–34]. We next tested how the repression of this accumulation affects mRNA chain elongation speed. When we knocked out a ppGpp synthetase gene (*relA*), we found that the Δ*relA* strain (NMK134) exhibited a higher speed than the WT strain under N starvation, although the difference was small (Fig. 3a and Supplementary Fig. 13). One possible reason for the small difference might be the presence of the other (p)ppGpp synthetase, SpoT. We next knocked out *spoT* (in the Δ*relA* background). However, the resulting (p)ppGpp-null strain did not grow in minimal medium, as previously reported[46]. Also, when we grew these cells in LB medium and then starved them, they lost viability immediately. Thus, we were not able to measure gene expression.

To overcome this problem, we constructed a strain that produces (p)ppGpp at a low level but does not accumulate it in massive amounts under starvation. We replaced the native P_{relA}-relA on the chromosome with P_{tac}-relA′ (cloned from pALS13 used above[45]) and the native *spoT* gene with *spoT-E319Q*, which contains a mutation that eliminated (p)ppGpp synthesis[47]; we designated this strain as NMK217. Because this strain grows at the same growth rate as WT at 10 μM IPTG (Supplementary Fig. 14), we maintained this IPTG concentration in the culture (note that our results regarding the effect of (p)ppGpp synthesis defect on gene expression do not depend on the specific IPTG concentration because the addition of other low IPTG concentrations yielded the same results; see Supplementary Fig. 15). This strain synthesizes (p)ppGpp constitutively (independently of starvation) but lacks the endogenous regulation that drives the abrupt accumulation of (p)ppGpp upon starvation. In this context, we referred to this strain as the (p)ppGpp-defective strain. We found that under N starvation, this strain exhibited much higher transcription elongation speeds than WT (Fig. 3a and Supplementary Fig. 13). Therefore, the repression of (p)ppGpp accumulation sped up transcription elongation. This observation agrees with our finding above that (p)ppGpp accumulation slows transcription elongation (Supplementary Fig. 12), establishing the (p)ppGpp-mediated slow-down of transcription elongation. (Currently, we do not know the molecular mechanism for this slow-down, and further studies are needed to address the mechanism; see Supplementary Fig. 16).

We next characterized how (p)ppGpp defect influences transcription–translation coordination under N starvation. Unable to slow transcription elongation, the (p)ppGpp-defective strain may not achieve the coordination in translation-limiting conditions, thereby exhibiting premature transcription termination. Our measurements of the mRNA copy number m_{head} and m_{tail} indeed revealed premature termination. Upon promoter induction, m_{head} in the (p)ppGpp-defective and WT strains increased similarly (Fig. 3b and Supplementary Fig. 17a), indicating that the (p)ppGpp defect did not affect promoter activity. However, m_{tail} in the defective strain remained zero (Fig. 3b and Supplementary Fig. 17a). This premature transcription termination is likely to impair protein synthesis. Indeed, this strain failed to produce LacZ proteins, in contrast with robust LacZ protein synthesis in the WT strain (Fig. 3c and Supplementary Fig. 18a). Collectively, these findings show that (p)ppGpp can affect gene expression kinetics without directly affecting promoter activity.

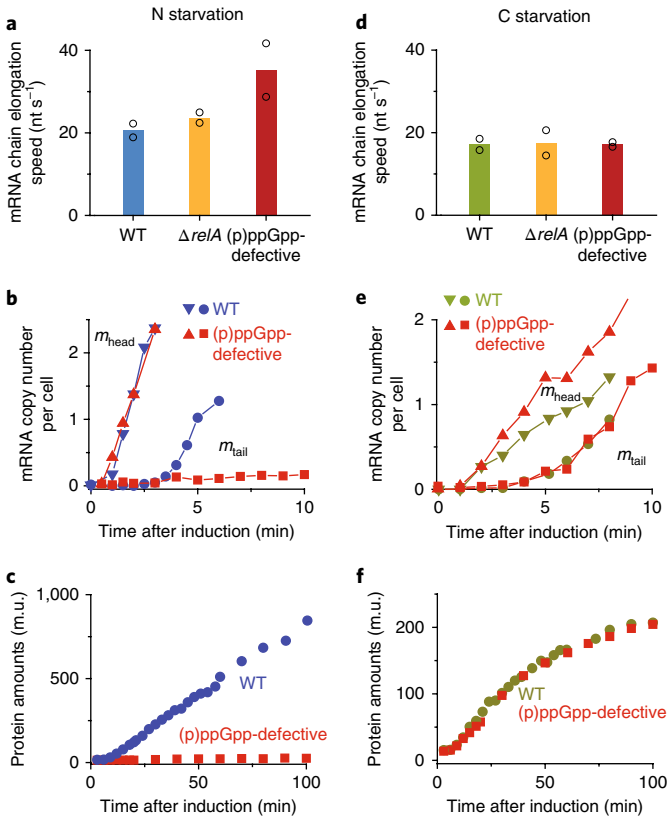

Fig. 3 | Contrasting effects of (p)ppGpp on transcription and translation kinetics under N- and C starvation. a, We determined *lacZ* mRNA chain elongation speeds under N starvation. When we performed a *t*-test, the two-tailed *P* value between the WT and Δ*relA* strains was 0.1739; hence, the difference is not statistically significant. The two-tailed *P* value between the WT and the defective strains was 0.0306, and hence the difference is statistically significant. Two biologically independent experiments were performed. The dots and bar show the data from the two independent experiments and their mean. **b**, We characterized m_{head} (blue inverse triangles) and m_{tail} (blue circles) of *lacZ* mRNA molecules in WT cells, and compared m_{head} (red triangles) and m_{tail} (red squares) of the (p)ppGpp-defective strain under N starvation. See Supplementary Note 3 for further discussion. Two biologically independent experiments were performed and we obtained very similar results. **c**, We characterized LacZ protein amounts under N starvation. Two biologically independent experiments were performed and we obtained very similar results. **d**, We determined *lacZ* mRNA chain elongation speeds under C starvation. When we performed a *t*-test, the two-tailed *P* value for the speeds between the WT and Δ*relA* strains and between the WT and (p)ppGpp-defective strains are respectively 0.8897 and 0.9917, and hence the differences are not statistically significant. See Supplementary Fig. 13 caption for why their speeds are expected to be similar. Two biologically independent experiments were performed. The dots and bar show the data from the two independent experiments and their mean. **e**, We characterized m_{head} (green inverse triangles) and m_{tail} (green circles) of *lacZ* mRNA molecules in WT cells, and compared m_{head} (red triangles) and m_{tail} (red squares) of the (p)ppGpp-defective strain under C starvation. Two biologically independent experiments were performed and we obtained very similar results. **f**, We characterized LacZ protein amounts under C starvation. Two biologically independent experiments were performed and we obtained very similar results. Note that all observations reported here were made using cells starved of nitrogen or carbon for 30 min. We made similar observations for cells starved for 10 min; see Supplementary Figs. 13, 17 and 18.

Under C starvation, (p)ppGpp is not needed for coordination between transcription and translation.. These detrimental effects of (p)ppGpp defect indicates an important role of (p)ppGpp as a coordinator. Yet, this role of (p)ppGpp is expected to be important only when translation is severely limited (N starvation). Under C starvation, transcription is severely limited, and the transcription-aid-translation mechanism is in effect. This mechanism naturally coordinates transcription to translation[9], alleviating the need of (p)ppGpp as a coordinator. Thus, we hypothesized that under C starvation, the (p)ppGpp synthesis defect is unlikely to cause the same detrimental effects observed under N starvation.

We tested this hypothesis by repeating the experiments using (p)ppGpp-defective strain under C starvation. Indeed, this strain produced full-length mRNAs and proteins as well as the WT strain; see similar increases in m_{head}, m_{tail} and LacZ amounts in Fig. 3e,f, and also Supplementary Figs. 17b and 18b. We then measured mRNA chain elongation speed (Fig. 3d and Supplementary Fig. 13b) and compared it with peptide chain elongation speed (this strain produced LacZ proteins under C starvation, making the measurement of the speed possible). We found that the mRNA chain elongation and peptide chain elongation speeds remained matched (Supplementary Fig. 19), indicating transcription–translation coordination; such coordination is expected given the lack of premature termination (Fig. 3e,f).

Condition-dependent effects of (p)ppGpp on the coordination extend to global gene expression activity and cellular adaptation.. Although we have thus far focused on *lacZ* expression, the observed condition-dependent effects of (p)ppGpp do not encompass any details specific to *lacZ*. Thus, these effects are expected to be non-specific, meaning that (p)ppGpp synthesis defect would disrupt global protein production under N starvation but not under C starvation. We tested this possibility by measuring the relative amounts of total proteins produced during starvation. We fluorescently labelled proteins newly synthesized during the first hour of starvation by using L-azidohomoalanine (AHA) and characterized the global protein synthesis activity; see Supplementary Fig. 20 caption and Methods for details. Even from a cursory visual inspection of the fluorescent protein gels (Supplementary Figs. 20 and 21), the condition dependence was evident; under N starvation, the fluorescence intensity of the (p)ppGpp-defective strain was much lower than that of the WT strain, whereas under C starvation they were similar. Quantitative determination of total intensities further confirmed this observation (Fig. 4a, b). This contrasting pattern for N- and C starvation, agreeing with the pattern we found for the LacZ protein (Fig. 3c,f), shows that the effect of (p)ppGpp on global protein synthesis is indeed condition-dependent.

Cellular adaptation to stressful environments depends critically on robust gene expression[5,12–14]. Therefore, the condition-dependent effects of (p)ppGpp on gene expression will have significant impacts on cell survival. We next examined the viability of the (p)ppGpp-defective and WT strains under starvation. Under N starvation, (p)ppGpp-defective cells lost their viability more rapidly than WT cells (Fig. 4c). Under C starvation, defective cells maintained their viability as well as did WT cells (Fig. 4d). Therefore, the condition-dependent effects of (p)ppGpp on gene expression were manifested in cell survival as well.

Discussion

In nature, bacteria frequently encounter stress. Extensive studies have focused on stress sensing and promoter regulation in bacteria[1]. This study focused on gene expression kinetics. We found that when transcription is severely limited (C starvation), translation aids transcription, and this aid mechanism naturally leads to their coordination. When translation is severely limited (N starvation), translation cannot aid transcription, and thus their coordination is no longer warranted. Instead, a coordinator that can slow down transcription elongation is needed. (p)ppGpp, an alarmone that

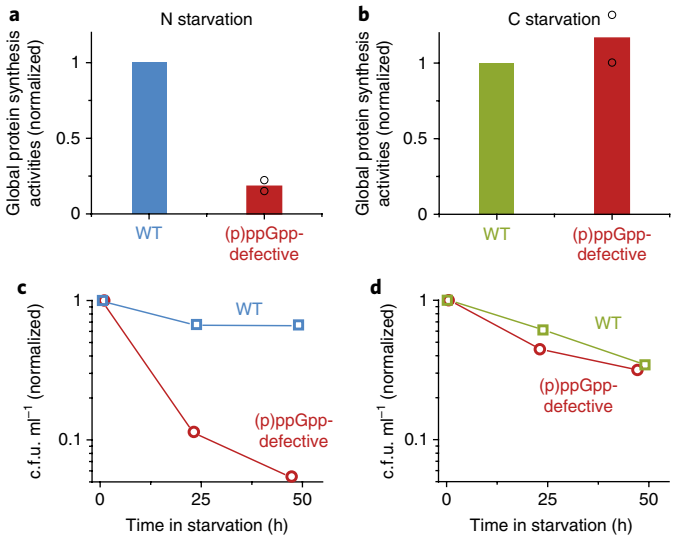

Fig. 4 | Condition-dependent effects of (p)ppGpp on global protein synthesis activity and cell survival. a,**b**, We fluorescently labelled amino acids in proteins newly synthesized during starvation and measured the total fluorescence intensities. See Supplementary Figs. 20 and 21 for fluorescent protein gels. Here, the total intensity reflects global protein synthesis activity. See text for details. We compared the global protein synthesis activities of the (p)ppGpp-defective and WT strains by plotting the total fluorescence intensities (normalized to the intensity of the WT strain). Two biologically independent experiments were performed. The dots and bar show the data from the two independent experiments and their mean. **c**,**d** We performed a conventional plating assay and determined the viability of the (p)ppGpp-defective and WT strains at various time points under N starvation (**c**) and under C starvation (**d**). Two biologically independent experiments were performed. We obtained very similar results from the two independent experiments. c.f.u., colony-forming units.

accumulates in cells under stress conditions, serves this role of coordinator. Importantly, in a transcription-limiting condition (C starvation), the natural coordination of transcription and translation alleviates the need for such a coordinator. This difference gives rise to condition-dependent involvement of (p)ppGpp in transcription–translation kinetics. Collectively, these findings reveal the kinetic aspect of gene expression plasticity.

We believe that our results advance understanding of (p)ppGpp function. Previous studies have extensively characterized its promoter regulation and identified the genes whose promoters are directly regulated by (p)ppGpp ((p)ppGpp regulon)[28,48]. To induce (p)ppGpp accumulation, these studies routinely starved *E. coli* cells of amino acids. Because *E. coli* cells are capable of synthesizing the amino acids they need from carbon and nitrogen sources, this amino acid starvation required auxotroph mutants or compounds that disrupt the incorporation of specific amino acids (for example, serine hydroxamate). Although this mode of starvation potently induces (p)ppGpp accumulation[32,33], it has severe side effects; it leads to ribosome stalling, disrupting the coordination of transcription and translation[27]. Hence, it is not ideal for studying the coordination of gene expression kinetics. Perhaps, this is why much less is known about the involvement of (p)ppGpp beyond promoter regulation.

Conversely, in nature, bacteria are often starved of carbon or nitrogen[11]. Our findings on nitrogen-starved cells establish (p)ppGpp as a kinetic coordinator, highlighting its importance on global gene expression. Interestingly, recent high-throughput studies reported that mutation repressing (p)ppGpp synthesis altered the expression of hundreds of other genes in addition to the known (p)ppGpp regulon[49], but mechanisms for this expansive effect remain unclear. Our findings may explain the reported findings. Furthermore, the comparison between nitrogen-starved and carbon-starved cells revealed the condition-dependent roles of (p)ppGpp as an effector of gene expression. More broadly, our finding that (p)ppGpp accumulation is critical for long-term survival under N starvation, but not under C starvation (Fig. 4c,d), highlights the significant implications of this role for cellular adaptation. Furthermore, a recent study found that nitrogen depletion directly activates *relA* expression[50]. Our findings that N-starved cells critically require (p)ppGpp for survival provide a rationale for this link.

Methods

Strains and cell culture. All strains were derived from *Escherichia coli* K12 strain NCM3722[51–53] and were listed in Supplementary Table 2. Details of strain construction are described in the Supplementary Information.

Cells were cultured at 37 °C with shaking at 250 r.p.m. in a water bath (New Brunswick Scientific). We monitored their growth by measuring the absorbance ($A_{600\,nm}$) of the culture (Genesys20 spectrophotometer, Thermo-Fisher with a standard cuvette (16.100-Q-10/Z8.5, Starna Cells Inc)). Our experimental procedure is as follows. *E. coli* cells were first seeded in LB media and cultured until they reached an $A_{600\,nm}$ of 1.0 (seed culture). Cells were diluted into 4 ml of N-C minimal media[54], supplemented with 20 mM of glycerol and 20 mM of ammonium chloride, and cultured overnight to the $A_{600\,nm}$ of 0.5 (pre-culture). Next morning, cells were diluted into 80 ml of N-C media to the $A_{600\,nm}$ of 0.01 (experimental culture). For experiments pertaining to carbon starvation, the N-C media were supplemented with 6 mM of glycerol and 20 mM of ammonium chloride (see Supplementary Fig. 3 caption for why we used glycerol, not glucose). With this supplementation, cells grew exponentially to the $A_{600\,nm}$ of 0.6 (Supplementary Fig. 3a); at this $A_{600\,nm}$, the carbon source (glycerol) became depleted and cell growth completely stopped[14]. For experiments pertaining to nitrogen starvation, cells were cultured in 20 mM of glycerol and 3 mM of ammonium chloride. With this supplementation, cells also grew exponentially to the $A_{600\,nm}$ of 0.6 (Supplementary Fig. 3b)[55]; at this $A_{600\,nm}$, the nitrogen source (ammonium) became depleted and cell growth stopped completely.

To activate the $P_{LTet\text{-}O1}$ promoter, 100 ng ml^{-1} of anhydrotetracycline (aTc) was added to cultures as soon as cell growth stopped, as described in the main text; 100 ng ml^{-1} leads to full induction of the promoter (Supplementary Fig. 2). Samples were collected at times indicated (10, 30 and 45 min after the onset of the starvation), and *lacZ* mRNA and protein levels were determined using the FISH assay and β-galactosidase assay. We also measured the mRNA and protein levels in cells exponentially growing in a nutrient-rich condition for comparison (for example, dashed lines in Fig. 1). The experimental procedure for the exponential-phase measurements were similar. The cells from the overnight pre-culture were diluted into 80 ml of the N-C media supplemented with 20 mM of glycerol and 20 mM of ammonium chloride, at the $A_{600\,nm}$ of 0.01. A bolus (100 ng ml^{-1}) of aTc was added to cultures immediately. We then allowed cells to grow to the $A_{600\,nm}$ of 0.6 and collected samples. As shown in Supplementary Fig. 22, mRNA levels increased immediately after the aTc addition, reaching the steady state levels within 5 min. After that point, mRNA levels stayed at constant levels. Thus, it is not critical exactly when the mRNA measurement was made (as long as the measurement was made after 5 min upon aTc addition).

To obtain the data presented in Fig. 2, we stopped translation elongation using chloramphenicol. We added chloramphenicol to cultures at the final concentration of 100 µg/ml, incubated for 5 minutes, added aTc, and collected samples at indicated time points for FISH measurement.

We used the strain NMK217 to control (p)ppGpp levels; see Supplementary Table 2. This strain harbours P_{tac}-relA′ on its chromosome. The response of the P_{tac} promoter to IPTG was shown to be sharp, leading to all-or-none induction[56,57]. If so, when the NMK217 strain was starved of nitrogen and treated with 10 µM IPTG, some cells might express *relA′* fully but other cells might not. If so, we would expect that some cells would produce the mRNA tails strongly while other cells would not. However, we did not observe such a heterogeneous response in our experiments.

Fluorescence in situ hybridization. The detail of the procedure was described in our recent article[15]. It is summarized below.

1. Probe labelling:

20–25 DNA probes that bind to 5′ and 3′ regions of the *lacZ* mRNA were designed using Stellaris software; see the reference[15] for the sequences of the probes. The sets of probes binding to the 5′ and 3′ end of the *lacZ* mRNA were labelled with ATTO 647 N NHS ester (ATTO-TEC GmbH, AD647-35) and 6-TAMRA NHS ester (Invitrogen, C6123), respectively. These dyes were chosen because they have distinct emission spectra. See Supplementary Table 4 and 5 for the exact locations where oligonucleotide probes bind and sequences of the probes.

2. Sample collection:

2.7 ml of cells was added to 300 µl of 37% (v/v) formaldehyde (Sigma). After incubating the cells in the formaldehyde solution for 30 min, the cells were spun down at 800*g* for 7 min. Cells were then washed twice using 1× PBS buffer. Finally,

the cells were re-suspended in 300 µl of DEPC-treated water, and 100% ethanol was added to the final volume of 1 ml.

3. Sample preparation:
Cells were spun down at 800*g* for 7 min and suspended in wash buffer (2× SSC buffer, 40% (w/v) formamide). Cells were spun down at 800*g* for 5 min and the supernatant was discarded. Cells were spun again at 800*g* and re-suspended in the hybridization buffer (2× SSC, 40% formamide, 0.1% w/v dextran sulfate, 10 mg tRNA and 0.1 % BSA and 0.5 mM ribonucleoside vanadyl complex). DNA probes labelled with fluorescent dyes were added to the cells to the final concentration of 120 nM and incubated overnight at 30 °C. The following day, 1 ml of wash buffer was added to the cell suspension and spun down at 800*g* for 7 min. The supernatant was discarded and the cell pellet was washed three times using the wash buffer to remove un-hybridized excess probes. Then, cells were re-suspended in 10 µl of 2× SSC buffer before imaging.

4. Microscope imaging and analysis: 4 µl of cell samples was placed on a 30 mm × 40 mm coverslip and covered with a 30 mm × 30 mm coverslip. The cells were then placed on the microscope (Olympus IX83P2Z) and imaged using a cooled cSMOS camera (Andor Neo). The best focal plane for imaging (z-position) was first determined using phase contrast. Nine fluorescence images were acquired at a Z-spacing of 300 nm. The images were analysed using a custom-built program (based on MATLAB).

Code availability. The custom-built program used for the analysis was described in our previous article[15]. This program is available and will be sent upon request.

β-Galactosidase assay. After induction by aTc, 110 µl of cell culture was collected at specified times and quick-frozen on dry ice. The β-galactosidase activity of each sample was measured using the traditional Miller method[58].

Fluorescent labelling of proteins using L-azidohomoalanine. We fluorescently labelled proteins newly synthesized during starvation using L-azidohomoalanine (AHA), an amino acid surrogate for L-methionine[59–61]. When added to the culture medium, AHA is incorporated into proteins in place of methionine. Subsequently, the AHA molecules can be fluorescently labelled using azide-alkyne click chemistry. Thus, the total fluorescence intensity reflects the total amount of new proteins produced. Our procedure is as follows.

Cells were grown as described above. We note that because we were interested in the endogenous activities of total protein expression, we did not induce LacZ expression from the $P_{LTet\text{-}O1}$ promoter in this experiment: thus, no aTc. AHA (Click Chemistry 1066) was added to the media, at the final concentration of 2 mM. (AHA was not added to the control samples). After 1 hour of incubation, cells were harvested and washed with chilled PBS buffer three times. Then, cell pellets were re-suspended in lysis buffer [50 mM Tris-HCl pH 8.0, 100 mM NaCl, 0.1% Triton X-100, 1× protease inhibitor cocktail (Sigma, P8849)] with lysozyme (1 mg ml^{-1}) and benzonase (>500 U). Pellets were incubated on ice for 30 min before being centrifuged at 20,000*g*. Bradford assay was performed to determine protein concentration in each sample[62]. The copper-catalysed click reaction of the samples with the Cy5.5 alkyne (Click Chemistry 1060) was performed using the Click Chemistry Protein Reaction Buffer Kit (Click Chemistry 1001) according to the manufacturer's manual. AHA-clicked proteins were then purified using methanol and chloroform. Protein pellets were re-suspended in 1× SDS sample buffer (the 4× SDS sample buffer contained 50 mM Tris-HCl pH 6.8, 2% SDS, 10 % glycerol, 1 % β-mercaptoethanol, 12.5 mM EDTA, 0.02% bromophenol blue). The samples were heated at 70 °C for 10 min, and the equal amounts of proteins were loaded to each lane in SDS–PAGE gels (protein concentration in each sample was determined before loading using Bradford assay[62]). The gels were visualized using the LI-COR Odyssey Fc imaging system (with the excitation wavelength of 700 nm). Finally, to confirm equal loading of proteins, coomassie blue staining (Thermo Fisher Scientific, G-250) was performed[63].

Data availability. The data obtained from this work are provided in Supplementary Table 1.

Received: 30 July 2017; Accepted: 16 April 2018;
Published online: 14 May 2018

References

1. Browning, D. F. & Busby, S. J. W. Local and global regulation of transcription initiation in bacteria. *Nat. Rev. Micro* **14**, 638–650 (2016).
2. Schellhorn, H. E. & Hassan, H. M. Transcriptional regulation of *katE* in *Escherichia coli* K-12. *J. Bacteriol* **170**, 4286–4292 (1988).
3. Santos, J. M., Lobo, M., Matos, A. P. A., De Pedro, M. A. & Arraiano, C. M. The gene *bolA* regulates dacA (PBP5), dacC (PBP6) and ampC (AmpC), promoting normal morphology in *Escherichia coli*. *Mol. Microbiol* **45**, 1729–1740 (2002).
4. Mengin-Lecreulx, D. & van Heijenoort, J. Effect of growth conditions on peptidoglycan content and cytoplasmic steps of its biosynthesis in *Escherichia coli*. *J. Bacteriol.* **163**, 208–212 (1985).
5. Matin, A., Auger, E. A., Blum, P. H., a. & Schultz, J. E. Genetic basis of starvation survival in nondifferentiating bacteria. *Annu. Rev. Microbiol.* **43**, 293–314 (1989).
6. Mellies, J., Wise, A. & Villarejo, M. Two different *Escherichia coli proP* promoters respond to osmotic and growth phase signals. *J. Bacteriol.* **177**, 144–151 (1995).
7. Yoshida, H., Yamamoto, H., Uchiumi, T. & Wada, A. RMF inactivates ribosomes by covering the peptidyl transferase centre and entrance of peptide exit tunnel. *Genes Cells* **9**, 271–278 (2004).
8. Cagliero, C. & Jin, D. J. Dissociation and re-association of RNA polymerase with DNA during osmotic stress response in *Escherichia coli*. *Nucleic Acids Res.* **41**, 315–326 (2013).
9. McGary, K. & Nudler, E. RNA polymerase and the ribosome: the close relationship. *Curr. Opin. Microbiol.* **16**, 112–117 (2013).
10. Ray-Soni, A., Bellecourt, M. J. & Landick, R. Mechanisms of bacterial transcription termination: all good things must end. *Annu. Rev. Biochem.* **85**, 319–347 (2016).
11. Morita, R. Y. *Bacteria in Oligotrophic Environments: Starvation-Survival Lifestyle* (Chapman & Hall, London, 1997).
12. Reeve, C. A., Amy, P. S. & Matin, A. Role of protein synthesis in the survival of carbon-starved *Escherichia coli* K-12. *J. Bacteriol.* **160**, 1041–1046 (1984).
13. Houser, J. R. et al. Controlled measurement and comparative analysis of cellular components in *E. coli* reveals broad regulatory changes in response to glucose starvation. *PLoS Comput. Biol.* **11**, e1004400 (2015).
14. Phaiboun, A., Zhang, Y., Park, B. & Kim, M. Survival kinetics of starving bacteria is biphasic and density-dependent. *PLoS Comput. Biol.* **11**, e1004198 (2015).
15. Iyer, S., Park, B. R. & Kim, M. Absolute quantitative measurement of transcriptional kinetic parameters in vivo. *Nucleic Acids Res.* **44**, e142 (2016).
16. Garcia, H. G., Lee, H. J., Boedicker, J. Q. & Phillips, R. Comparison and calibration of different reporters for quantitative analysis of gene expression. *Biophys. J.* **101**, 535–544 (2011).
17. Bremer, H. & Dennis, P. Modulation of chemical composition and other parameters of the cell at different exponential growth rates. *EcoSal Plus* https://doi.org/10.1128/ecosal.5.2.3 (2008).
18. Proshkin, S., Rahmouni, A. R., Mironov, A. & Nudler, E. Cooperation between translating ribosomes and RNA polymerase in transcription elongation. *Science* **328**, 504–508 (2010).
19. Kepes, A. Transcription and translation in the lactose operon of *Escherichia coli* studied by in vivo kinetics. *Progress. Biophys. Mol. Biol.* **19**, 199–236 (1969).
20. Schleif, R., Hess, W., Finkelstein, S. & Ellis, D. Induction kinetics of the l-arabinose operon of *Escherichia coli*. *J. Bacteriol.* **115**, 9–14 (1973).
21. Jin, D. J., Burgess, R. R., Richardson, J. P. & Gross, C. A. Termination efficiency at rho-dependent terminators depends on kinetic coupling between RNA polymerase and rho. *Proc. Natl Acad. Sci. USA* **89**, 1453–1457 (1992).
22. Dai, X. et al. Reduction of translating ribosomes enables Escherichia coli to maintain elongation rates during slow growth. *Nat. Microbiol* **2**, 16231 (2016).
23. Komissarova, N. & Kashlev, M. RNA polymerase switches between inactivated and activated states by translocating back and forth along the DNA and the RNA. *J. Biol. Chem.* **272**, 15329–15338 (1997).
24. Nudler, E., Mustaev, A., Goldfarb, A. & Lukhtanov, E. The RNA–DNA hybrid maintains the register of transcription by preventing backtracking of RNA polymerase. *Cell* **89**, 33–41 (1997).
25. Mamata, S. & Stefan, K. Backtracking dynamics of RNA polymerase: pausing and error correction. *J. Phys. Condens. Matter* **25**, 374104 (2013).
26. Steitz, T. A. A structural understanding of the dynamic ribosome machine. *Nat. Rev. Mol. Cell Biol.* **9**, 242–253 (2008).
27. Zhang, Y. et al. *DksA* guards elongating RNA polymerase against ribosome-stalling-induced arrest. *Mol. Cell* **53**, 766–778 (2014).
28. Potrykus, K. & Cashel, M. (p)ppGpp: still magical? *Annu. Rev. Microbiol.* **62**, 35–51 (2008).
29. Villadsen, I. S. & Michelsen, O. Regulation of PRPP and nucleoside tri and tetraphosphate pools in Escherichia coli under conditions of nitrogen starvation. *J. Bacteriol.* **130**, 136–143 (1977).
30. Metzger, S., Schreiber, G., Aizenman, E., Cashel, M. & Glaser, G. Characterization of the *relA1* mutation and a comparison of *relA1* with new *relA* null alleles in *Escherichia coli*. *J. Biol. Chem.* **264**, 21146–21152 (1989).
31. Gentry, D. R. & Cashel, M. Mutational analysis of the *Escherichia coli spoT* gene identifies distinct but overlapping regions involved in ppGpp synthesis and degradation. *Mol. Microbiol.* **19**, 1373–1384 (1996).
32. Ryals, J., Little, R. & Bremer, H. Control of rRNA and tRNA syntheses in *Escherichia coli* by guanosine tetraphosphate. *J. Bacteriol.* **151**, 1261–1268 (1982).
33. Cashel, M. & Gallant, J. Two compounds implicated in the function of the RC gene of *Escherichia coli*. *Nature* **221**, 838–841 (1969).
34. Spira, B., Silberstein, N. & Yagil, E. Guanosine 3',5'-bispyrophosphate (ppGpp) synthesis in cells of *Escherichia coli* starved for Pi. *J. Bacteriol.* **177**, 4053–4058 (1995).

35. Kingston, R. E., Nierman, W. C. & Chamberlin, M. J. A direct effect of guanosine tetraphosphate on pausing of *Escherichia coli* RNA polymerase during RNA chain elongation. *J. Biol. Chem.* **256**, 2787–2797 (1981).
36. Kingston, R. E. & Chamberlin, M. J. Pausing and attenuation of in vitro transcription in the rrnB operon of E. coli. *Cell* **27**, 523–531 (1981).
37. Krohn, M. & Wagner, R. Transcriptional pausing of RNA polymerase in the presence of guanosine tetraphosphate depends on the promoter and gene sequence. *J. Biol. Chem.* **271**, 23884–23894 (1996).
38. Vogel, U., Sørensen, M., Pedersen, S., Jensen, K. F. & Kilstrup, M. Decreasing transcription elongation rate in *Escherichia coli* exposed to amino acid starvation. *Mol. Microbiol.* **6**, 2191–2200 (1992).
39. Sørensen, M. A., Jensen, K. F. & Pedersen, S. High concentrations of ppGpp decrease the RNA chain growth rate. *J. Mol. Biol.* **236**, 441–454 (1994).
40. van Ooyen, A. J. J., Gruber, M. & Jørgensen, P. The mechanism of action of ppGpp on rRNA synthesis in vitro. *Cell* **8**, 123–128 (1976).
41. Barker, M. M., Gaal, T., Josaitis, C. A. & Gourse, R. L. Mechanism of regulation of transcription initiation by ppGpp. I. Effects of ppGpp on transcription initiation in vivo and in vitro. *J. Mol. Biol.* **305**, 673–688 (2001).
42. Travers, A. A. Promoter sequence for stringent control of bacterial ribonucleic acid synthesis. *J. Bacteriol.* **141**, 973–976 (1980).
43. Ross, W. et al. ppGpp binding to a site at the RNAP-DksA interface accounts for its dramatic effects on transcription initiation during the stringent response. *Mol. Cell* **62**, 811–823 (2016).
44. Roghanian, M., Zenkin, N. & Yuzenkova, Y. Bacterial global regulators DksA/ppGpp increase fidelity of transcription. *Nucleic Acids Res.* **43**, 1529–1536 (2015).
45. Svitil, A. L., Cashel, M. & Zyskind, J. W. Guanosine tetraphosphate inhibits protein synthesis in vivo. A possible protective mechanism for starvation stress in *Escherichia coli*. *J. Biol. Chem.* **268**, 2307–2311 (1993).
46. Xiao, H. et al. Residual guanosine 3',5'-bispyrophosphate synthetic activity of relA null mutants can be eliminated by spoT null mutations. *J. Biol. Chem.* **266**, 5980–5990 (1991).
47. Harinarayanan, R., Murphy, H. & Cashel, M. Synthetic growth phenotypes of *Escherichia coli* lacking ppGpp and *transketolase A* (*tktA*) are due to ppGpp-mediated transcriptional regulation of tktB. *Mol. Microbiol.* **69**, 882–894 (2008).
48. Haugen, S. P., Ross, W. & Gourse, R. L. Advances in bacterial promoter recognition and its control by factors that do not bind DNA. *Nat. Rev. Micro.* **6**, 507–519 (2008).
49. Durfee, T., Hansen, A.-M., Zhi, H., Blattner, F. R. & Jin, D. J. Transcription profiling of the stringent response in *Escherichia coli*. *J. Bacteriol.* **190**, 1084–1096 (2008).
50. Brown, D. R., Barton, G., Pan, Z., Buck, M. & Wigneshweraraj, S. Nitrogen stress response and stringent response are coupled in *Escherichia coli*. *Nat. Commun.* **5**, 4115 (2014).
51. Soupene, E. et al. Physiological studies of *Escherichia coli* strain MG1655: growth defects and apparent cross-regulation of gene expression. *J. Bacteriol.* **185**, 5611–5626 (2003).
52. Lyons, E., Freeling, M., Kustu, S. & Inwood, W. Using genomic sequencing for classical genetics in *E. coli* K12. *PLoS ONE* **6**, e16717 (2011).
53. Brown, S. D. & Jun, S. Complete genome sequence of *Escherichia coli* NCM3722. *Genome Announc.* **3** (2015).
54. Csonka, L. N., Ikeda, T. P., Fletcher, S. A. & Kustu, S. The accumulation of glutamate is necessary for optimal growth of *Salmonella typhimurium* in media of high osmolality but not induction of the proU operon. *J. Bacteriol.* **176**, 6324–6333 (1994).
55. Kim, M., Zhang, Z. G., Okano, H., Yan, D. L., Groisman, A. & Hwa, T. Need-based activation of ammonium uptake in Escherichia coli. *Mol. Syst. Biol.* **8**, 616 (2012).
56. Novick, A. & Weiner, M. Enzyme induction as an all-or-none phenomenon. *Proc. Natl Acad. Sci. USA* **43**, 553–566 (1957).
57. Kuhlman, T., Zhang, Z., Saier, M. H. Jr & Hwa, T. Combinatorial transcriptional control of the lactose operon of *Escherichia coli*. *Proc. Natl Acad. Sci. USA* **104**, 6043–6048 (2007).
58. Miller, J. H. *Experiments in Molecular Genetics* (Cold Spring Harbor Laboratory Press, New York, 1972).
59. Dieterich, D. C., Link, A. J., Graumann, J., Tirrell, D. A. & Schuman, E. M. Selective identification of newly synthesized proteins in mammalian cells using bioorthogonal noncanonical amino acid tagging (BONCAT). *Proc. Natl Acad. Sci. USA* **103**, 9482–9487 (2006).
60. Beatty, K. E. et al. Live-cell imaging of cellular proteins by a strain-promoted azide–alkyne cycloaddition. *ChemBioChem* **11**, 2092–2095 (2010).
61. Hatzenpichler, R. et al. In situ visualization of newly synthesized proteins in environmental microbes using amino acid tagging and click chemistry. *Environ. Microbiol.* **16**, 2568–2590 (2014).
62. Bradford, M. M. A rapid and sensitive method for the quantitation of microgram quantities of protein utilizing the principle of protein-dye binding. *Anal. Biochem.* **72**, 248–254 (1976).
63. Merril, C. R. Gel-staining techniques. *Methods Enzymol.* **182**, 477–488 (1990).

Acknowledgements

We thank M. Cashel, R.L. Gourse and J. Wang for helpful discussions and kindly sharing strains with us. This work was funded by Research Corporation for Science Advancement (24097) and the Human Frontier Science Program (RGY0072/2015).

Author contributions

S.I., D.L., B.R.P. and M.K. designed the study. S.I., D.L. and B.R.P. performed experiments. S.I. D.K. and B.R.P. analysed the data. M.K. wrote the manuscript.

Competing interests

The authors declare no competing interests.

Additional information

Supplementary information is available for this paper at https://doi.org/10.1038/s41564-018-0161-3.

Reprints and permissions information is available at www.nature.com/reprints.

Correspondence and requests for materials should be addressed to M.K.

Publisher's note: Springer Nature remains neutral with regard to jurisdictional claims in published maps and institutional affiliations.